Permafrost and Periglacial Processes

WILEY

RESEARCH ARTICLE OPEN ACCESS

A Multimethod Investigation of the Lake Agnes Rock Glacier, Colorado, USA

Brianna Rick[1,2] | Daniel McGrath[1] | Benjamin Lehmann[3] | Timothy Fegel[4] | Keith Williams[5] | Suzanne Anderson[3]

[1]Department of Geosciences, Colorado State University, Fort Collins, Colorado, USA | [2]Alaska Climate Adaptation Science Center, Fairbanks, Alaska, USA | [3]INSTAAR and Department of Geological Sciences, University of Colorado Boulder, Boulder, Colorado, USA | [4]Rocky Mountain Research Station, USDA Forest Service, Fort Collins, Colorado, USA | [5]UNAVCO, Inc., Boulder, Colorado, USA

Correspondence: Brianna Rick (brianna.rick@colostate.edu)

Received: 9 March 2023 | **Revised:** 2 July 2024 | **Accepted:** 2 November 2024

Funding: This material is based upon work supported by the National Science Foundation Graduate Research Fellowship awarded to B.R. under Grant No. 006784-00002, as well as funding awarded to B.R. by the American Alpine Club, the Geological Survey of America, and the Tobacco Root Geological Society. B.L. thanks the Mobility fellowship P2LAP2_191400 from the Swiss National Science Foundation for their support.

Keywords: hydrochemistry | hydrology | rock glacier

ABSTRACT

Rock glaciers are important headwater landforms that play a key role in alpine hydrology. North American rock glaciers are estimated to contain the third largest water volume equivalent globally, and over 3800 rock glaciers have been mapped in Colorado alone. However, these features are often overlooked in alpine water budgets. In this study, we present initial results using geophysical, hydrochemical, and repeat structure from motion data to investigate the ice presence, downslope movement, and influence on stream chemistry of the Lake Agnes rock glacier in the northern Front Range, Colorado, USA. We measured an average velocity of $23 \pm 4\,\text{cm year}^{-1}$ in the upper 400 m of the rock glacier, with maximum velocities up to $36 \pm 4\,\text{cm year}^{-1}$. Rock glacier–fed streams ($n = 2$) near the spring remained below 2.5°C throughout the summer, mixed-source streams ($n = 3$) remained below 3.5°C, and a non–rock glacier stream ($n = 1$) reached 13.5°C. Rock glacier streams additionally recorded elevated ion concentrations and pH relative to the mixed-source and lake–fed streams. Geophysical surveys suggest that the rock glacier has an internal structure consisting of a ~3-m-thick active layer, underlain by an ice-poor layer up to 10 m thick and by an ice-rich layer up to 18 m thick, with total rock glacier thickness between 20 and 30 m. This study supports the presence of ice within the Lake Agnes rock glacier and documents the rock glacier's influence on basin hydrochemistry. In many basins, including Lake Agnes, the reduced climate sensitivity of rock glaciers and their sustained cold-water input to mountain streams will likely provide a refuge for cold-water species in a warming climate.

1 | Introduction

Rising air temperatures impact glaciers, snowpack, snowmelt timing, and stream temperatures, influencing the presence and survival of certain cold-water alpine species [1–4]. As glaciers disappear, particularly in the Southern Rocky Mountains, ground ice—such as is present within active rock glaciers—will likely play a greater role in maintaining cold streams in a warming climate. Thick debris cover dampens melt rates and insulates ground ice, providing a refuge for species dependent on cold water streams for habitat, from microbial communities to aquatic macroinvertebrates to fish [2, 5–9]. However, these long-term sources of cold water are relatively understudied and are often not considered as future water resources [10–16].

Rock glaciers are lobate- or tongue-shaped debris landforms created by current or former permafrost creep and found in mountain environments [17–19]. Rock glaciers have a range of morphologies, dictated by slope, glaciological setting, and climatic controls [5, 12, 20]. A rock glacier of glacial origin generally has a core with massive ice and is considered to be the end member of the glacier—debris-covered glacier—rock glacier continuum [5, 21, 22]. The periglacial model describes how interstitial ice or ice lenses form from freezing rain, meltwater, groundwater, and/or snow and ice accumulations, which are buried by rock and eventually induce permafrost creep [12, 23–26]. These two origin models have varying internal rock glacier structures (massive glacial ice vs. interstitial ice) that aid in interpreting origin as well as ice content (with massive ice estimated to have a higher percent ice content) for hydrological estimations and runoff implications [12].

Rock glaciers can be difficult to study because of their coarse, blocky, and unstable surfaces that conceal ice beneath the surface. Geophysical surveys allow for subsurface interpretation and are the main tool used to estimate rock glacier depth to ice, bedrock, and internal structure [13, 27–31]. For example, ground-penetrating radar (GPR) can help determine whether a rock glacier is composed of massive or interstitial ice, the depth of the active layer, and internal layers [27, 31, 32]. Seismic refraction is similarly used to identify internal structure based on changes in seismic velocity that correspond to changes in material (e.g., rock and air in the active layer, ice or rock and ice mixture, and bedrock; [29, 30]). The thick surface debris layer, which makes rock glaciers difficult to study, is also what makes them more resilient to warming temperatures, as the debris partially insulates the ice from external climate forcings [5, 33]. Active rock glaciers are able to persist even when the environmental equilibrium line altitude is above their maximum elevations, and some ground ice has persisted throughout the Holocene [5, 34–36].

The presence or absence of a rock glacier or permafrost within a basin can impact short-, intermediate-, and long-term water storage because of impacts on snowmelt and precipitation runoff, seasonal ice melt, and internal ice melt [37, 38]. In the La Sal Mountains, Utah, rock glaciers were found to act as an impervious surface and increase runoff from alpine basins, representing 15%–30% of total basin runoff [37]. Work in the Green Lakes Valley, Colorado, documented a substantial contribution of rock glaciers to late summer/early fall (September–October) streamflow and an increase in late season discharge over a ~30-year timespan (1982–2009; [39]). Water samples from a rock glacier stream in the Uinta Mountains, Utah, were aged from 0 to 2 years, suggesting that both snowmelt/annual ice melt and ice from the rock glacier interior contributed to streamflow [14]. Water chemistry from a rock glacier in the Austrian Alps also supports a combination of snowmelt, internal ice melt, and precipitation contributing to streamflow throughout the summer [40]. These studies illustrate the importance of hydrological contributions from rock glaciers, particularly to late-season discharge.

In addition, streamflow characteristics and water chemistry are important in determining ecosystem function and capacity [41–43]. Rock glaciers contribute significantly to the biogeochemistry of alpine headwaters and support a higher microbial richness and diversity than clean ice glaciers [41]. Rock glacier streams from intact rock glaciers (i.e., have internal ice) tend to have elevated ion concentrations as well as lower temperatures as compared with non–rock glacier basins, although specific ion concentrations are mountain range or even basin specific, and are dependent on local lithology [14, 39, 41, 43]. Rock glaciers that maintain even very low discharge streams late in the summer can sustain aquatic life where ephemeral streams may not [2]. In certain basins, the reduced climate sensitivity of rock glaciers and their sustained cold-water input to mountain streams could mitigate the predicted habitat loss for endemic species [2, 6–9, 44].

Colorado is home to over 3800 rock glaciers, vastly outnumbering the ~16 glaciers present today [45]. Rock glaciers cover a much larger spatial extent, occupying nearly 13 times more area in the Front Range than glaciers [46]. Previous studies in Colorado have documented displacement rates, hydrological impacts, and internal structure of a few individual rock glaciers, though these studies are limited spatially and temporally. Photogrammetric analysis documented average horizontal rock glacier velocities from 14 to 20 cm year^{-1} in the Front Range [47], whereas in situ measurements ranged from 5 to 10 cm year^{-1} [48, 49]. Displacement in rock glaciers indicates ice presence, which has been confirmed in the Green Lake 5 rock glacier through geophysical surveys, observing a depth of 4–5 m of the active layer and a total rock glacier thickness of 16–18 m [13, 50]. This ice presence also influences basin hydrology, with water draining from this same rock glacier rarely exceeding 2.5°C [50], and rock glacier baseflow constituting 38% of the hydrograph between June and October [43]. Late-season streamflow in Green Lakes Valley increased between 1982 and 2009, likely because of the melting of permafrost ice [39]. Although the Green Lakes Valley has received concentrated attention, few studies have examined the spatial and temporal distribution of rock glacier influence on basin hydrology elsewhere in Colorado and the western United States.

In the present study, we incorporated geophysical, hydrochemical, and repeat uncrewed aerial vehicle (UAV) structure from motion (SfM) data to investigate the ice presence, displacement rate, and hydrologic influence of the Lake Agnes rock glacier in the northern Front Range, Colorado. Although rock glacier influence varies between individual landforms, a case study of the Lake Agnes rock glacier expands the scarce data available concerning the status and role of rock glaciers in alpine watersheds within the western United States.

2 | Study Area

The Lake Agnes rock glacier is located in a north-facing cirque within the Never Summer Mountains of northern Colorado, USA (40°28′34.14″N, 105°54′8.22″W; Figure 1). The rock glacier is 0.16 km^2, is 700 m long, ranges in elevation from 3260 to 3525 m asl with an average slope of 30°, and is classified as active [45, 46]. The rock glacier itself is composed of at least two distinct units, with geomorphological evidence of an active unit in the upper 400 m, overriding an inactive or relic unit in the lower 300 m. The nearest long-term weather station is the Joe Wright SNOTEL station (site 551), located 6.2 km northeast of Lake Agnes at 3096-m elevation. At this site, the mean annual air temperature is 1.51°C and the mean annual precipitation is

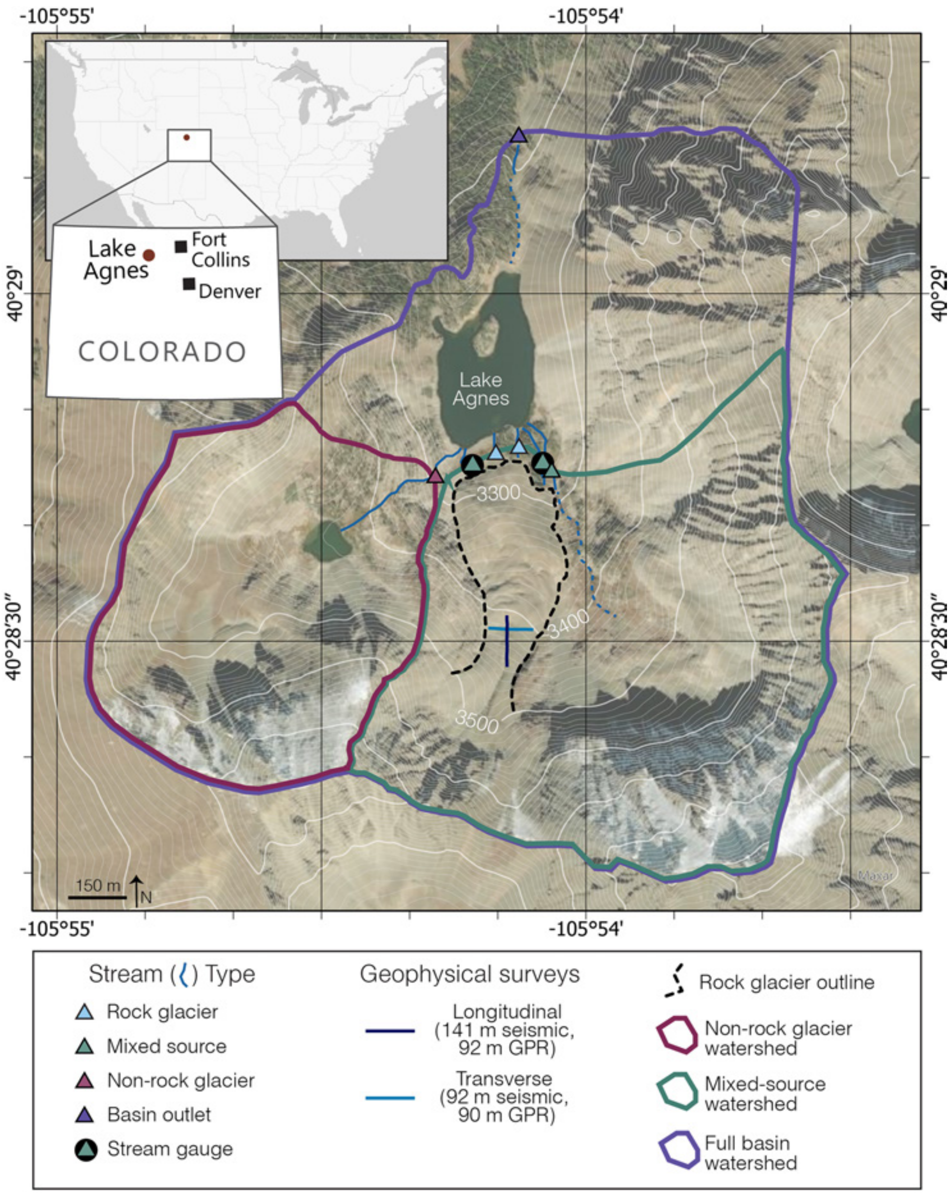

FIGURE 1 | Location of the Lake Agnes rock glacier with watersheds outlined for the non–rock glacier (plum), mixed-source (green), and basin outlet (purple) streams (basemap provided by ESRI, 2022; contours produced from USGS, 2021). The location of geophysical surveys (blue lines) and stream sites (triangles) are also present. Dark blue lines represent streams, with dashed lines indicating intermittent or below-surface streams. [Colour figure can be viewed at wileyonlinelibrary.com]

1132 mm (from 1981 to 2018; [51]). The landcover within the Lake Agnes catchment is mainly exposed rock, with patches of vegetation (shrubs, grasses) surrounding the shores of Lake Agnes. The surrounding bedrock and rock glacier source material are granodiorite of Miocene age, with principal minerals of andesine, potassium feldspar, quartz, hornblende, biotite, and minor pyroxene [52]. Talus slopes additionally exist beneath the headwalls of the cirques and could contain small amounts of permafrost ice.

The study area is grouped into three main basins: (1) the non–rock glacier basin (0.7 km^2, mean slope = 29°, mean aspect = 162°); (2) the mixed basin (1.2 km^2, 14% rock glacier coverage, mean slope = 33°, mean aspect = 232°); and (3) the full basin (2.7 km^2, 6% rock glacier coverage, mean slope = 32°, mean aspect = 209°), which encompasses Basins 1 and 2, as well as Lake Agnes (0.1 km^2) (Figure 1). The non–rock glacier basin contains three small protalus ramparts that are minimally to moderately active [45] and a small lake (0.01 km^2) that feeds the non–rock glacier stream. Protalus ramparts additionally line the bottom of the headwall in the southeast portion of the mixed basin.

Lake Agnes is located 4 km west of the Continental Divide, draining naturally as a headwater into the North Platte Basin. However, Lake Agnes is also the headwaters of the Michigan Ditch. This transmountain diversion moves nearly 3 million cubic meters of water from the North Platte Basin to the Poudre River annually, supplying water to the Joe Wright Reservoir, which stores and supplies water for communities along Colorado's Front Range (NSOS, 2017). Consequently, Lake Agnes is an important headwater for both the North Platte Basin and the Poudre River Basin.

3 | Methods

This study incorporates geophysical, hydrochemical, and remotely sensed data from June to October 2019, 2020, and 2021 to investigate the ice presence, movement, and hydrologic contribution to late-season streamflow from the Lake Agnes rock glacier (Figure 2). Field campaigns in late summer 2020 were impacted by the Cameron Peak fire [53] as the field site was inaccessible.

3.1 | Water Quality and Streamflow

A total of 78 water samples were collected and filtered in situ (0.45-μm Restek Syringe filters) at seven stream locations (two pure rock glacier, three mixed-source, one non–rock glacier, and one basin outlet; Figure 2) throughout the 2019, 2020, and 2021 snowmelt and snow-free time periods (see Figure 5 for sample dates). Samples were refrigerated and stored in air-tight containers

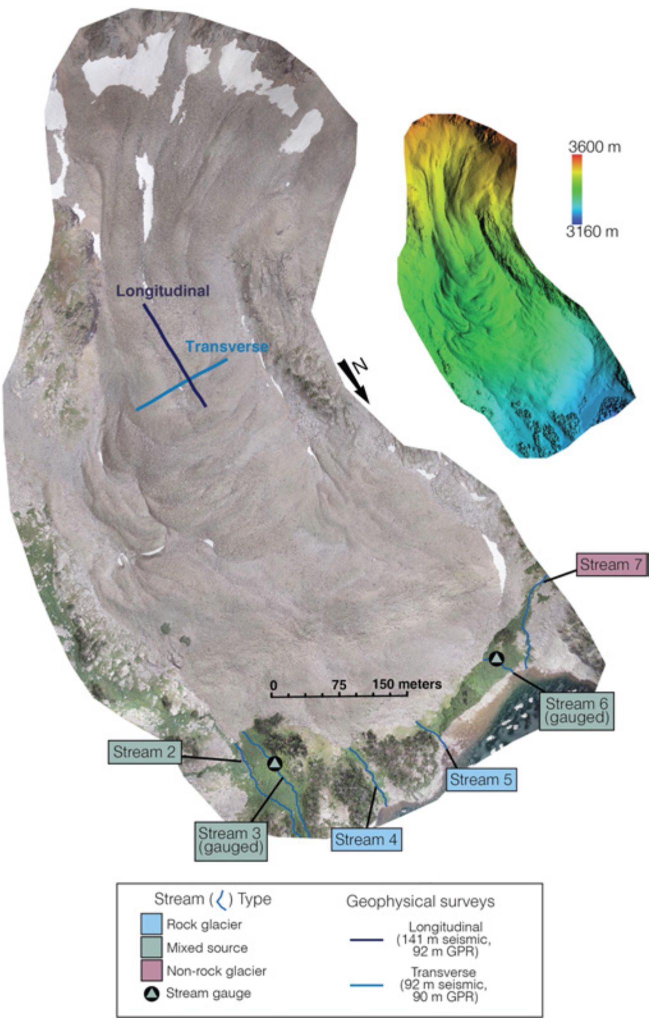

FIGURE 2 | Summary of locations of sampled streams with stream type and geophysical surveys. The upper right shows the hillshade derived from the digital elevation model, colored by the elevation of the rock glacier derived from the UAV survey on August 31, 2019. Note that the basin outlet sampling site is not shown in this figure—see Figure 1 for location. The orthoimage was produced from the UAV survey on August 31, 2019. [Colour figure can be viewed at wileyonlinelibrary.com]

until they were processed for stable isotopes (δ^2H and $\delta^{18}O$) in 2019 at the University of Wyoming Stable Isotopes Lab and in 2020–2021 at the Colorado State University NREL EcoCore Lab. Ion concentrations were analyzed at the Rocky Mountain Research Station's Biogeochemistry Lab (Ca^{2+}, Mg^{2+}, Na^{+}, K^{+}, NH_4^{+}, Cl-, NO_3-, PO_4^{3-}, SO_4^{2-}) via ion chromatography. Water temperature, pH, and electrical conductivity (EC) were collected in situ using a handheld sensor (Apera PC400S) at the time of sampling. Rock glacier and mixed-source streams were measured within 30 m of the spring. Two stream gauges (TruTrack WT-HR data logger) recorded stream stage at 15-min intervals at mixed-source streams (Streams 3 and 6; Figure 2) draining the rock glacier and upper basin throughout the snow-free period.

In situ discharge measurements were collected using the tracer dilution method [54]. By conducting these measurements at different stream heights, we created a rating curve to convert the stage record into a hydrograph for each gauge location (Figure S1). A total of seven manual discharge measurements were used to create the rating curve for the stream gauge at the eastern rock glacier outflow (Stream 3; $R^2=0.99$), and five measurements were used for the western rock glacier outflow (Stream 6; $R^2=0.99$; Figure S1).

3.2 | Geophysics: Seismic Refraction and GPR

Geophysical techniques are well-established for gathering information about the internal structure of rock glaciers [29]. GPR measures variations in dielectric properties, and for rock glaciers specifically, these properties vary for air, ice, and rock. Seismic refraction tomography (SRT) uses changes in seismic velocity to infer internal layering. Typically, rock glacier structure consists of a surface layer of rock and air (the active layer during unfrozen conditions) with P-wave velocities ranging 500–1500 m/s, a heterogenous layer of rock and ice with intermediate velocities ranging ~3000–4000 m/s, an unfrozen, fine-grained layer, and then bedrock below with high velocities (> 4500 m/s), although velocities are dependent on rock type and ice content [29, 30].

Two seismic refraction surveys were conducted in October 2019 using a Geometrics Geode Exploration Seismograph 24-channel data acquisition system, one longitudinal profile (141 m, 3 m geophone spacing), and one transverse to flow (92 m, 4 m geophone spacing). After removing the spikes, the 4.5-Hz geophones were attached directly to boulders using plumber's putty to increase contact. The energy source was a 5-kg sledgehammer hit against a metal plate, and traces were stacked eight times per location to improve the signal-to-noise ratio. First arrivals were manually picked, and the data were inverted using Geogiga Seismic Pro software (Version 9.0), with inversion velocities constrained between 300 and 6000 m/s.

We used Sensors & Software DVL 500 and PulseEkko Pro 100 MHz antennas [27, 31] to conduct GPR surveys in common-offset configuration to survey two transects coinciding with the seismic transects in July 2020. Antennas were separated by 1 m, and traces were collected every 0.25 m, with a time-sampling interval of 100 ps and 32 stacks at each survey location. An Emlid Reach RS2 RTK multiconstellation GNSS system was used for geolocating

GPR traces for the longitudinal line, and GNSS points were collected every 10 m along the transverse line. The slight discrepancy in elevation profiles for GPR and SRT is likely due to small horizontal offsets during surveys to find more suitable ground.

Radargrams were processed in ReflexW software (Version 9.0; Sandmeier Geophysical Research, 2019) with the following steps: (1) move start time, (2) dewow filter, (3) divergence compensation, (4) butterworth bandpass filter, and (5) running average filter. An assumed electromagnetic wave velocity of 0.13 m/ns was chosen based on previous studies working in a similar environment [32, 55].

One electrical resistivity survey was attempted using a SuperSting-R8 for an along-flow profile (167 m, 3 m spacing), but poor coupling between electrodes and boulders resulted in frequent high voltage errors and insufficient data collection. Placing saline water-soaked sponges between electrodes and boulders [29] did not improve coupling sufficiently to produce usable data.

3.3 | SfM

UAV surveys were conducted on August 31, 2019, and September 24, 2021, using a DJI Phantom Pro 4 and DJI Mavic Pro 2, respectively. Flights were planned using Pix4Dcapture and flown in a double grid pattern with 80% overlap and at an average height of 73 m above the surface. Ground control points (GCPs; $n = 10$; 0.05-m accuracy) consisted of 1-m square black and white targets. An additional four "natural" GCPs (e.g., distinct rock fractures, corners, and features; see Figure S2) were used for consistency and coregistration between years. Agisoft Metashape software (Version 1.7.6) was used to process images ($n = 555$ for 2019, $n = 1797$ for 2021) from each acquisition date for SfM. During processing, the raw images were first filtered by image quality (> 0.6) and then aligned with a bundle adjustment using default settings for key point and tie point limits. Low-quality points were filtered from the model using a reconstruction uncertainty (geometry) of 10.0 and a projection accuracy (pixel matching errors) of 3.0. GCP coordinates were imported and manually identified on each image where the GCP was visible. A camera optimization was then run to improve the location estimates of the cameras. A high-quality dense point cloud was then created and used to create a digital elevation model and orthomosaic for each of the surveyed years. To improve the alignment between images for displacement calculations, all products were coregistered to the 2019 orthomosaic using stable areas such as bedrock. Center coordinates for GCPs were measured using two Emlid Reach RS2 GNSS units (one as a base station and one as a rover) for a postprocessed kinematic (PPK) survey. Postprocessing was performed using the RTK Library and documentation (RTKLib version 2.4.3 [56]).

Orthomosaics from 2019 (2.3 cm per pixel) and 2021 (1.8 cm per pixel) were used to estimate 2D horizontal displacement using the feature-tracking IMCORR module [57] within the SAGA toolbox in QGIS [58]. This module identifies pixel patterns between two georeferenced images and estimates displacement between small subsections of the images. We used the following parameters within IMCORR: a search window size of 128 × 128 pixels, a reference window size of 64 × 64 pixels, and a grid spacing of 1 m. Displacement within stable control areas (i.e., bedrock) should be the accumulation of error from producing the orthomosaics as well as the image correlation process. As these stable areas should not have moved within the 2-year time period, we use the median value of calculated displacement within control areas (0.04 m) as the bias between orthoimages and can be considered the detection limit. Therefore, areas showing a surface displacement lower than 0.04 m are considered below the detection level.

4 | Results

4.1 | Water Quality and Streamflow

Hydrochemical results (pH, temperature, ion concentrations, $\delta^{18}O$) of stream samples distinguish between rock glacier, non–rock glacier, and mixed-source streams (Figure 3). Rock glacier–fed streams (measured within 30 m of the spring) were statistically different ($p < 0.05$) from the other stream types with elevated Na^+, Mg^{2+}, Ca^+, K^+, SO_4^{2-}, EC, and pH, whereas stream temperatures remained low (< 2.5°C) throughout the summer. The non–rock glacier stream maintained low EC throughout the summer, never exceeding 40 μS/cm. Conversely, rock glacier streams were statistically different ($p < 0.05$) from all other streams with consistently high EC values (> 100 μS/cm). The mixed-source streams and basin outlet recorded increasing values throughout the summer, with a maximum of 85 and 58 μS/cm in October, respectively. Rock glacier streams were slightly more alkaline than the other streams with a median pH of 8.1, whereas the median pH for non–rock glacier, mixed, and outlet streams were 7.6, 7.5, and 7.6, respectively.

The non–rock glacier stream experienced seasonal temperature variation, increasing from 1.8°C during snowmelt to 13.5°C in August 2021 (Figure 3). The basin outlet stream also had seasonal variations in temperatures, ranging from 1.8°C to 8.6°C. The mixed-source streams ranged in temperatures from 0.6°C to 3.5°C, whereas the rock glacier streams ranged from 0.6°C to 2.5°C.

The $\delta^{18}O$ from the rock glacier streams displayed little variation throughout the year, with values ranging between −17.3‰ and −16.0‰ (Figure 4). The basin outlet showed a similar range in $\delta^{18}O$ values. The mixed-source and non–rock glacier streams both had depleted $\delta^{18}O$ values early in the summer during snowmelt (~−18‰), similar to the values observed in the rock glacier stream and basin outlet. However, the mixed-source and non–rock glacier stream $\delta^{18}O$ values increased throughout the summer (reaching ~−15‰). The values for both the non–rock glacier and outlet streams deviate in slope from the global meteoric water line (GMWL), whereas the mixed-source and rock glacier streams maintain the GMWL slope (Figure 4B).

Discharge from mixed-source Streams 3 and 6 exhibits seasonal and annual variability in runoff, influenced by snowpack, snowmelt, and precipitation (Figure 5). Stream 3 had consistently greater discharge in 2020 and 2021 (an average of 3.7 times higher in July), although diurnal oscillations in Stream 6 in the second half of July in 2019 exceeded the discharge of Stream 3. Stream 3 had low yet persistent flow throughout the entire summer, whereas Stream 6 ran dry in

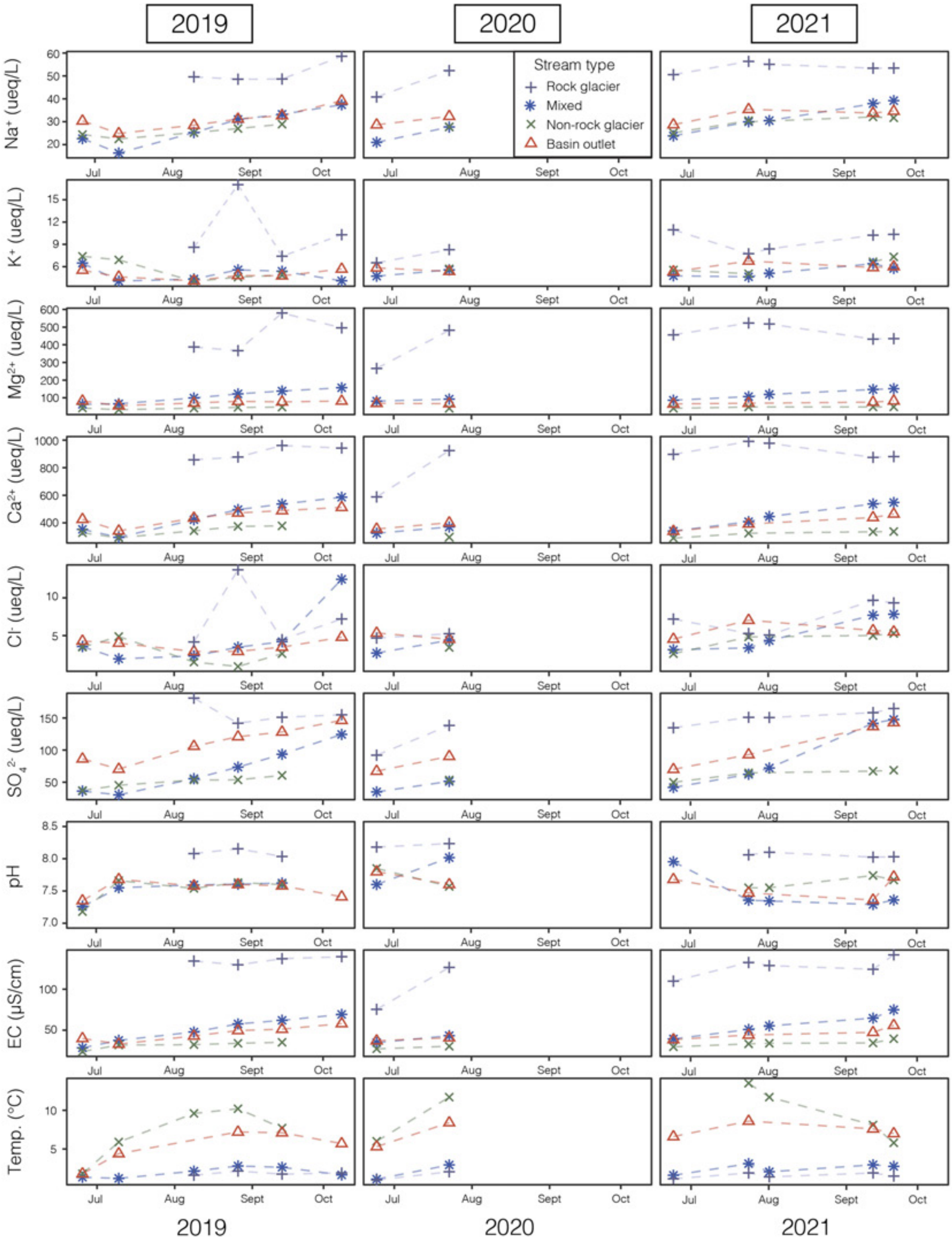

FIGURE 3 | Time series for 2019, 2020, and 2021 of water quality for rock glacier, non–rock glacier, mixed-source, and basin outlet streams. Values for the two rock glacier and two mixed-source streams were averaged per sample date. EC stands for electrical conductivity. We were unable to collect water samples in August, September, and October 2020 because of the nearby Cameron Peak fire. [Colour figure can be viewed at wileyonlinelibrary.com]

late September and early October in 2020 and 2021. However, Stream 6 is a short reach (approximately 30 m between the front of the rock glacier and the lake) with boulders (up to ~70-cm diameter) such that flow could be heard subsurface even when the surface stream was dry. Discharge in the second half of July was the greatest in 2019, followed by 2020, then 2021, reflected by the July snow cover in the Lake Agnes basin (Figure 6).

4.2 | Geophysics: Seismic Refraction and GPR

The seismic velocity model estimated for the upper lobe of the Lake Agnes rock glacier is composed of a low-velocity layer adjacent to the surface with velocities ranging from 300 to 2000 m/s (Zone 1), a medium-velocity layer beneath this with velocities ranging from 2000 to 3500 m/s (Zone 2), and a high-velocity layer even deeper with velocities of > 4000 m/s (Zone 3; Figure 7). In the longitudinal

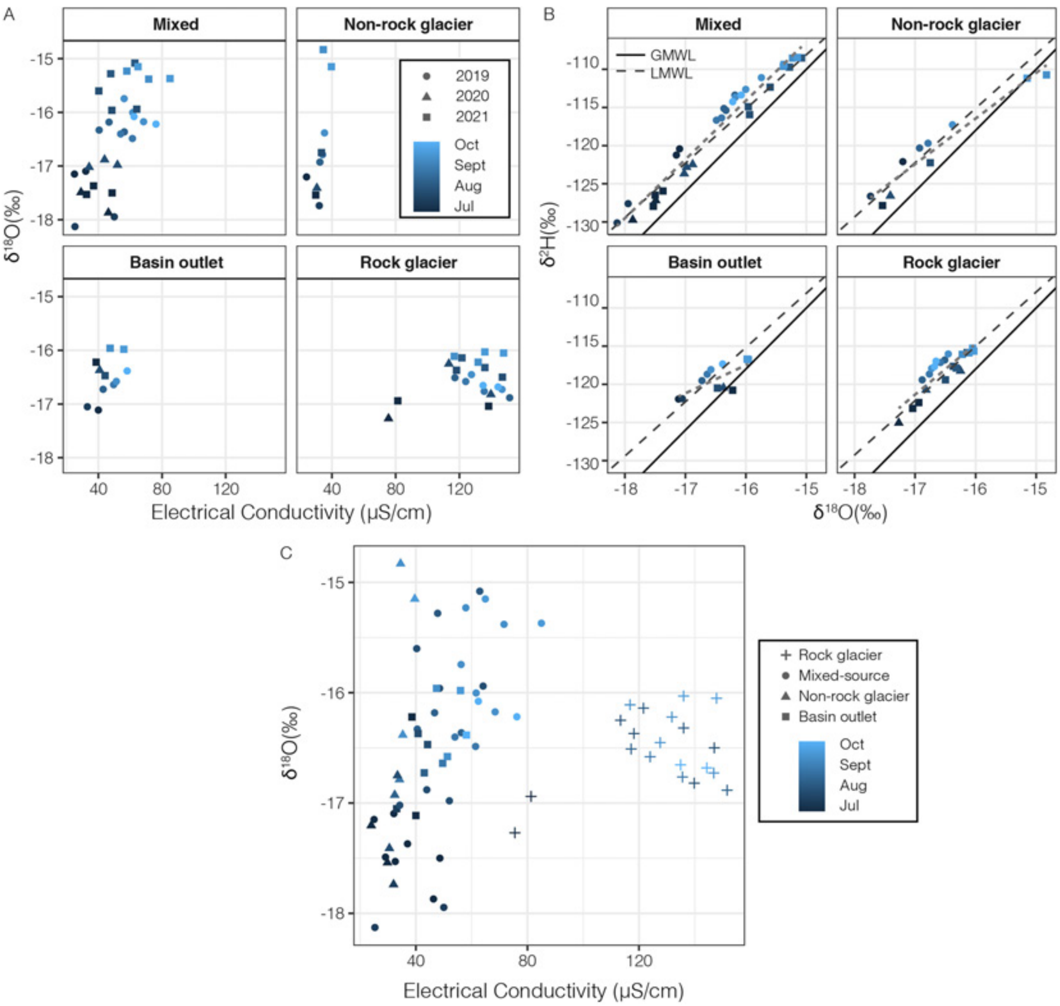

FIGURE 4 | Electrical conductivity vs $\delta^{18}O$ values for all water samples (A), separated by stream type and colored by date collected, with shape representing the year the sample was collected. $\delta^{18}O$ versus $\delta^{2}H$ values for all water samples (B), separated by stream type and colored by date collected, with shape representing the year the sample was collected. The solid line represents the global meteoric water line (GMWL), the black dashed line is the local meteoric water line (LMWL), and the gray dashed shows the slope for each stream type. Electrical conductivity versus $\delta^{18}O$ values for all water samples (C), colored by month of the year that the sample was collected, with shape representing the stream type. [Colour figure can be viewed at wileyonlinelibrary.com]

profile, the low-velocity layer ranges in thickness from 4 at 42 m along the profile to 10 at 70 m along the profile. From 36 to 64 m along the profile, a high-velocity layer is indicated about 8–10 m below the surface. However, this high-velocity layer is not identified from 0 to 36 m and 70–141 m along the profile.

In the transverse profile, the seismic profile follows a similar structure, with a low-velocity layer (Zone 1) consistently ~3 m thick, though this layer thickens to ~6 m from 20 to 30 m along the profile as well as from 74 to 88 m along the profile. The higher velocity (> 4000 m/s; Zone 3) layer appears between 48 and 66 m along the profile at about 12-m depth.

The longitudinal GPR radargram is characterized by a relatively consistent reflector at 3-m depth, underlain by a layer containing many reflectors to about 10-m depth. Below this is a zone where reflectors are of a much lower magnitude. This package is underlain by a high magnitude reflector at 30-m depth seen from 74 to 96 m along the profile and is interpreted as the bottom of the rock glacier.

The transverse GPR radargram is similarly characterized by a relatively consistent reflector at 3-m depth, underlain by a layer containing many reflectors, followed by a layer of low-magnitude reflectors. A strong reflector is identified at ~20-m depth from 0 to 10 m and 63–70 m along the profile and at ~15-m depth from 79 to 89 m along the profile. The estimated rock glacier thickness at the east end of transverse line of ~20 m corresponds to the elevation difference measured between the off-glacier and the start of the line as measured using a DEM. A furrow is present in the transect at about 45 m along the profile, with topography that was too challenging to collect GPR traces. At 20 m along the profile is the top of a small ridge, with shallow, downward-dipping reflectors angled away from the high point roughly parallel to the surface slope.

4.3 | SfM

Rock glacier displacements between the 2019 (RMSE = 5 cm) and 2021 (RMSE = 4.5 cm) orthomosaics (both resampled to 2.5 cm

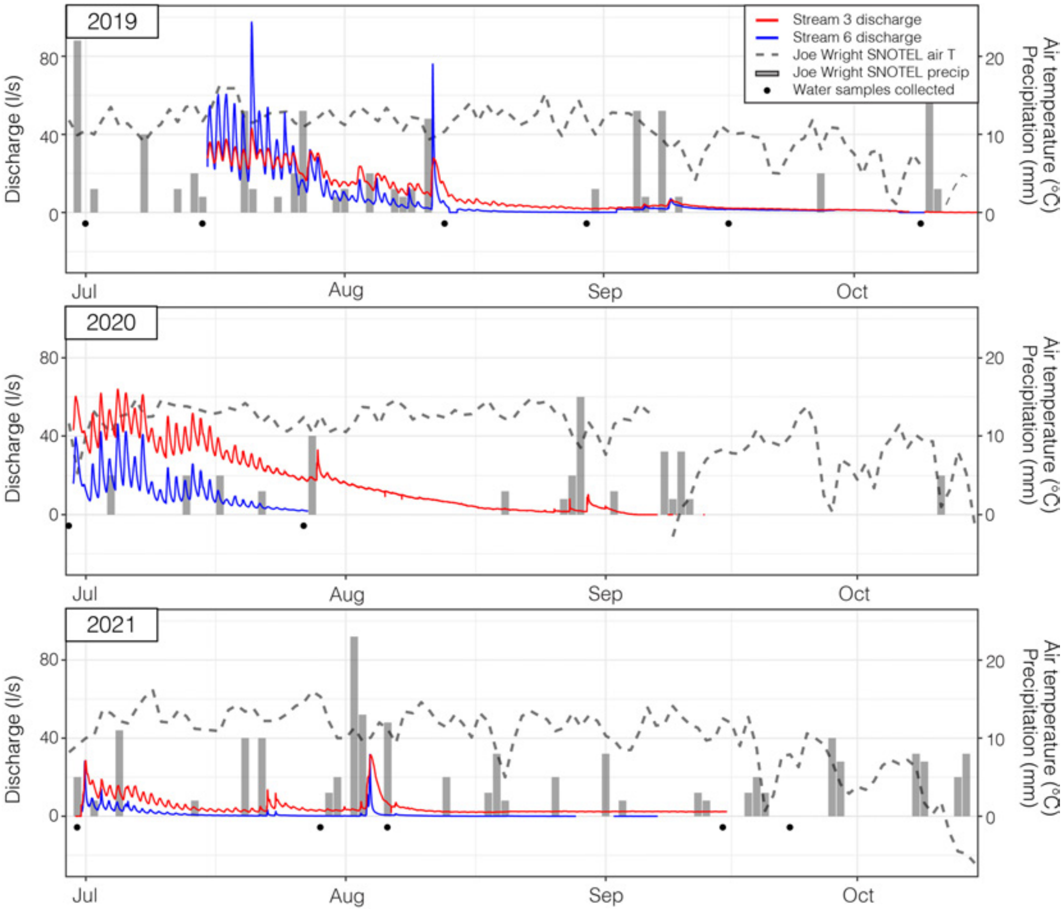

FIGURE 5 | Discharge (l/s) from mixed-source Streams 3 (red) and 6 (blue) from June 29 to October 15 in 2019 (top), 2020 (middle), and 2021 (bottom). Gray bars represent precipitation (mm) recorded at the Joe Wright SNOTEL site, located 6.2 km away. The dashed line represents the mean daily air temperature (°C) recorded at the Joe Wright SNOTEL site. Black dots indicate when water samples were collected each year. [Colour figure can be viewed at wileyonlinelibrary.com]

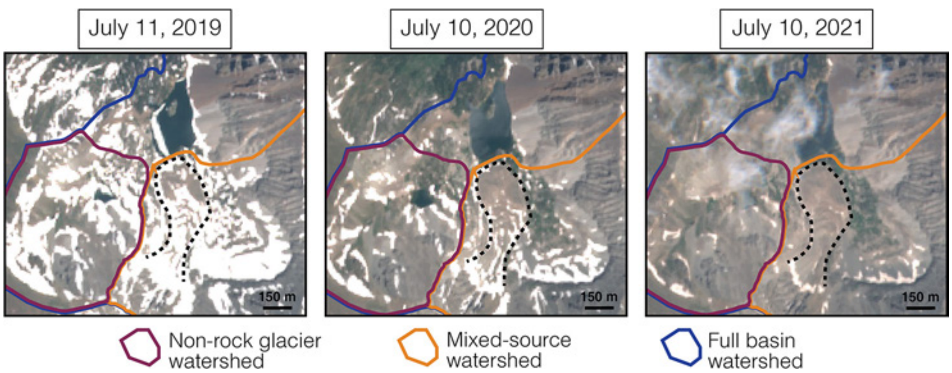

FIGURE 6 | Sentinel-2 satellite imagery from July 11, 2019, July 10, 2020, and July 10, 2021, comparing snow cover in the Lake Agnes basin. The rock glacier is outlined by a black dashed line. The non–rock glacier (magenta), mixed-source (orange), and full basin (blue) watersheds are also outlined. [Colour figure can be viewed at wileyonlinelibrary.com]

per pixel) confirm movement in the upper 400 m of the rock glacier, whereas the lower half of the landform experiences little to no detectable movement (Figure 8A). The average horizontal velocity of the active rock glacier unit was 23 ± 4 cm year^{-1}, with maximum velocities up to 36 ± 4 cm year^{-1}. The median velocity over areas of stable bedrock was 4 cm year^{-1}, and therefore, this value was used as the bias for the velocity calculated between the 2 years.

5 | Discussion

5.1 | Geochemistry

Elevated ion concentrations in rock glacier–sourced streams draining the Lake Agnes rock glacier are consistent with previous studies [14, 39, 41, 43, 59]. The elevated ions are likely sourced from groundwater within the rock glacier and have

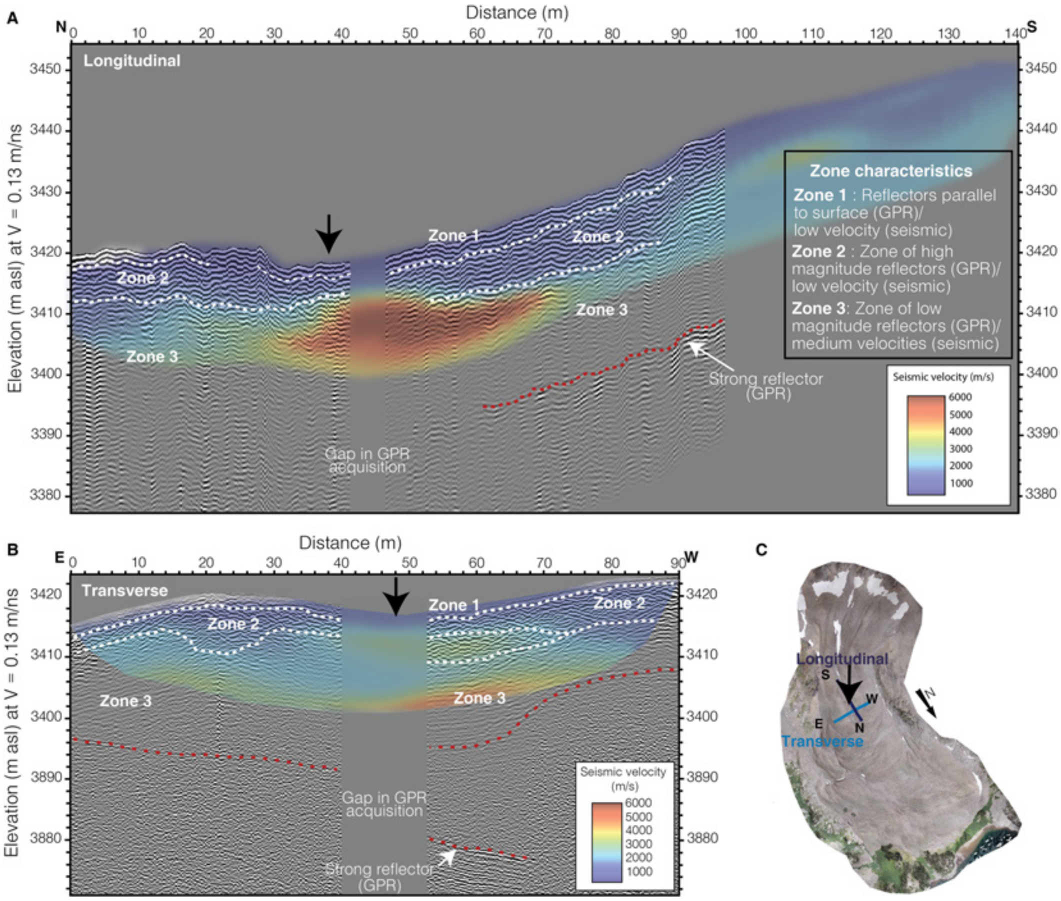

FIGURE 7 | Seismic velocity models overlain upon GPR radargrams for longitudinal (A) and transverse profiles (B) on the Lake Agnes rock glacier (C). The black arrows indicate where the two lines intersect. The white dashed line delineates layers within the rock glacier, and the red dashed lines outline other strong reflectors at depth. See Figure S4 for unannotated radargrams. [Colour figure can be viewed at wileyonlinelibrary.com]

been proposed to be sourced from atmospheric fallout during previous cold periods [60, 61]. Elevated weathering products can also, at least partially, be explained through the breakdown of the source material, granodiorite, a rock composed mostly of Na- and Ca-rich feldspars. Substantial contact between rock surfaces and ice within the rock glacier can increase chemical weathering [62], and although rock glacier creep might enhance mechanical weathering, the low velocities of the Lake Agnes rock glacier indicate that abrasion is likely limited.

The oxygen isotope values for both the non–rock glacier and outlet streams deviate in slope from the GMWL, whereas the mixed-source and rock glacier streams maintain the GMWL slope. This suggests that the non–rock glacier and outlet streams have evaporative influence, particularly later in the summer. Both streams are located beneath lakes where this evaporation likely occurs. Because the rock glacier streams do not show evidence of evaporation, the higher ion concentrations cannot be attributed to evaporative processes. The shift in oxygen isotope values in the mixed and non–rock glacier streams from early to late in the summer likely reflects the changing proportion of snowmelt (depleted $\delta^{18}O$ values) to precipitation and groundwater (more enriched $\delta^{18}O$ values).

Using EC as a proxy for the sum of ion concentrations, rock glacier–fed streams sustained relatively high concentrations throughout the summer (mean = 129 μS/cm), whereas the non–rock glacier–sourced stream remained low (< 40 μS/cm). The increasing EC throughout the season for mixed-source and basin outlet streams suggests an increase in groundwater contribution toward the end of the summer. In addition, the Lake Agnes rock glacier plays an important role in maintaining low temperatures throughout the summer. The non–rock glacier–fed stream reached a maximum temperature of 13.5°C, whereas the maximum temperature recorded near the rock glacier spring was 2.5°C. The mixed streams recorded a maximum temperature of 3.6°C, implying that the rock glacier reduced the maximum water temperature by 10°C, a large decrease during the peak heat of summer. However, it is important to note that the non–rock glacier stream is located beneath a small lake, which likely influences the thermal regime of the stream. Regardless, rock glaciers elsewhere in North America have recorded a similar muting of summer stream temperature increases, though this muting can be spatially limited depending on the downstream environment [14, 32, 33, 43]. For example, the streams sourced from the Lake Agnes rock glacier flow directly into Lake Agnes and only provide a maximum of 200 m of cold-water habitat.

The two mixed-source stream hydrographs in the Lake Agnes basin exhibited similar behavior to rock glacier–fed alpine streams in the La Sal Mountains, Utah [37], with large diurnal fluctuations during snowmelt, followed by low flow with muted diurnal fluctuations and large peaks following precipitation events. The low

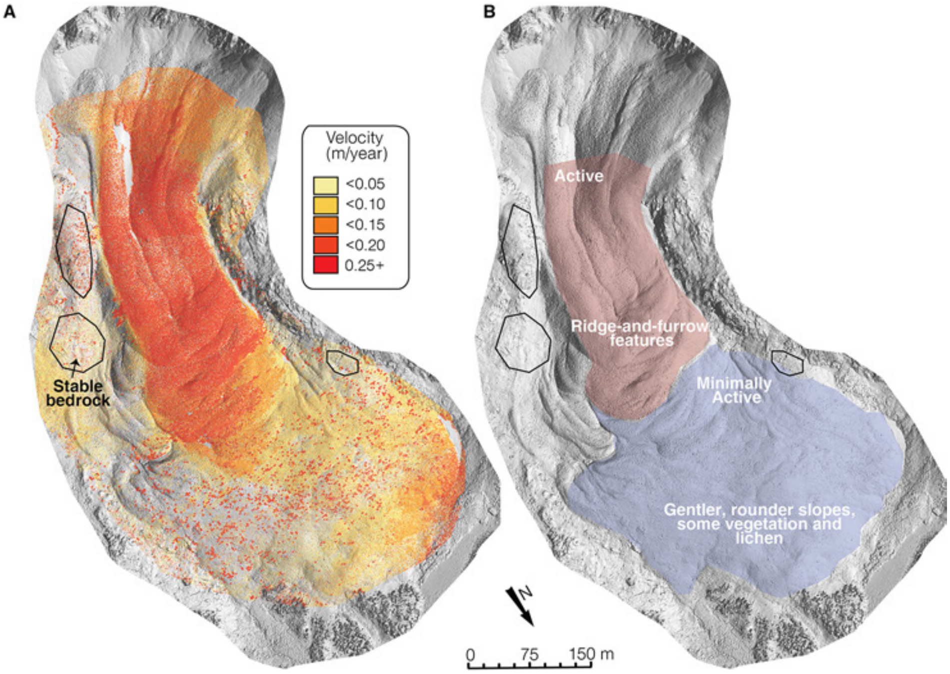

FIGURE 8 | Rock glacier velocities calculated between 2019 and 2021 (A), shown in meters per year. A mask was applied to remove displacement from vegetation growth and snow loss. See Figure S3 for displacement vectors. The geomorphology (B) of the Lake Agnes rock glacier corresponds to the active and minimally active lobes of the rock glacier. Stable bedrock control areas are outlined in black. [Colour figure can be viewed at wileyonlinelibrary.com]

temperatures, in conjunction with minimal diurnal fluctuations, found within the rock glacier–fed and mixed-source streams could create a stable environment for cold-water aquatic communities to thrive. Elevated rock glacier meltwater solute concentrations can impact biological community assemblages and therefore change the characteristics of the water chemistry in alpine watersheds [43]. These key differences make it possible to distinguish meltwater sourced from rock glaciers and are important in determining ecosystem function and capacity.

5.2 | Horizontal Velocity

A photogrammetric study of rock glaciers in the Front Range found that long-term velocities averaged between 14 and 20 cm year^{-1} from 1978 to 1999 [47], and this rate is within uncertainty of what we observed at the Lake Agnes rock glacier (2019–2021; Figure 7). The average rate of the active Lake Agnes lobe (upper ~ 400 m), 25 ± 7 cm year^{-1}, is higher than InSAR-derived velocities in the Uinta Mountains, Utah, which ranged from 0.4 to 6 cm year^{-1} [63]. Slower velocities found in the middle of the upper tongue could be due to more complex 3-D deformation that is not captured in simple horizontal displacements (i.e., if rocks are moving up or down a ridge). The lower magnitude of movement in the lower half of the Lake Agnes rock glacier indicates that although the upper half of the rock glacier is active, the bottom half is better classified as transitional [19]. The displacement of the rock glacier confirms the presence of ice within the upper reaches of the rock glacier, supported by the geomorphology of steep ridge and furrow features and a steep lateral margin (40°) on the eastern side of the upper rock glacier (Figure 8B). This presence of ice within the landform has implications for short-, intermediate-, and long-term water storage.

5.3 | Rock Glacier Structure

Seismic refraction and GPR results provide insight into the internal structure of the upper portion of the Lake Agnes rock glacier, and by combining the seismic tomography with interpretations from radargrams, we can reduce some ambiguities associated with these geophysical methods, though ambiguities remain. The geophysical results suggest a typical layered structure to the upper lobe, with a ~3 m top layer of slow velocities interpreted to be the active layer composed of large rocks and air space observed in both longitudinal and transverse profiles. Beneath the active layer is a sequence of reflectors with high magnitude, underlain by a package with weak reflectivity, interpreted to be a layer of low ice content transitioning to high ice content [13]. This package of weak reflectivity is characterized by intermediate seismic velocities ranging from 2000 to 4500 m/s, consistent with permafrost layers observed in other rock glaciers as well [29, 32]. It is unlikely that the frozen layer sits directly on bedrock, but rather transitions to a layer of unfrozen sediment just above the bedrock.

Unlike the radargrams of the Galena Creek rock glacier, Wyoming, USA [31], we did not see a massive layer devoid of reflectors (i.e., limited variation in dielectric properties) indicating a high purity glacial ice core. The radargrams for the Lake Agnes rock glacier look similar to that of the Green Lake 5 rock glacier [13], and thus, the less reflective zone is likely debris with ice or very high ice content. A borehole would be beneficial to aid in interpretation [29, 64], but unfortunately, this is not logistically feasible at this site. The upper lobe thickness is estimated to be ~20 m in the transverse profile, with thickness up to 30 m in the longitudinal profile. The high seismic velocities (> 4500 m/s) indicated from 40 to 64 m along the longitudinal profile suggest that bedrock is present 8–10 m below the surface.

This could indicate the thinning of the rock glacier as it flows up and over a bedrock topographic high point. However, the seismic velocity model and radargram are inconsistent in this area, making interpretation ambiguous.

5.4 | Hydrological Impacts of the Rock Glacier

Geophysical surveys and remote sensing confirm the presence of ice within the Lake Agnes rock glacier, whereas hydrochemical measurements document the impact of this ice on streams within the basin. By comparing rock glacier-sourced streams to non–rock glacier-sourced streams, we conclude that the Lake Agnes rock glacier increases ion concentrations and pH while maintaining streams < 2.5°C during the snow-free period.

Streamflow characteristics and water chemistry are important in determining ecosystem function and capacity and therefore influence the presence and survival of alpine species. Biologists have recently identified the importance of "icy seeps" (i.e., rock glacier–fed streams) in maintaining aquatic biodiversity in alpine basins and creating a cold-water refuge for species in a warming climate [9, 41, 42, 65]. Rock glaciers are important headwater features in a deglaciating world, with a delayed response to current and future warming. Catchments containing rock glaciers, such as Lake Agnes, are predicted to dampen the impacts of warming temperatures for as long as these features persist [12].

Colorado is home to over 3800 rock glaciers, with over 90% of these features classified as active [45]. These landforms total 363 km^2 and are abundant at high elevations, ranging from 2328 to 4066 m asl (median of 3600 m asl). As indicated by the Lake Agnes rock glacier, these features can have important hydrological implications that are rarely considered in alpine hydrology. Further study is needed to fully understand how rock glaciers impact alpine hydrology and habitat at a regional scale.

5.5 | Limitations and Future Work

This study serves as a first investigation into the setting and characteristics of the Lake Agnes rock glacier, exploring which measurements are viable and providing useful information to better understand the rock glacier system. The large, coarse, blocky surface with subsurface voids provided a challenging environment for geophysical surveys. An electrical resistivity survey yielded no usable data due to electrode coupling difficulties, and the GPR and seismic refraction lines were limited by the challenging surface topography. Site access and the Cameron Peak fire in 2020 limited the frequency of water samples collected. Low streamflow and streambed geometry rendered the pure rock glacier streams unsuitable for a stream gage, whereas a rocky streambed and often subsurface flow of the non–rock glacier stream made it also unsuitable for a stream gage. This limited our ability to compare runoff between the different stream types.

Valuable future work could include continuous water quality measurements to fully capture seasonal variation and response to precipitation events, full rock glacier geophysical surveys to better understand ice presence within the lower half of the rock glacier as well as storage capacity, and continuous GPS measurements to capture seasonal velocity variations. Additional stream gages in the rock glacier and non–rock glacier–fed streams and sampling from Little Lake Agnes (above the non–rock glacier stream) would also help to characterize the hydrologic influence of the rock glacier within this basin. Stable isotope measurements from snow, precipitation, and rock glacier ice would enable analysis of a mixing model to better understand the sources for water in each of the streams.

6 | Conclusions

This study improves our knowledge of the Lake Agnes rock glacier and provides a framework for studying the thousands of other rock glaciers in Colorado and the western United States, to better understand the extent and influence of subterranean ice in alpine ecosystems. We confirm the presence of ice within the Lake Agnes rock glacier and document its influence on basin hydrochemistry, elevating ion concentrations, pH, and maintaining low stream temperatures. We estimate an active layer depth of ~3 m and a total rock glacier thickness of 20–30 m. We measured an average velocity of $23 \pm 4\ cm\ year^{-1}$ between 2019 and 2021 for the active lobe. The data collected here add to the sparse record of rock glacier hydrochemistry, particularly for regions outside of the European Alps. In certain basins, the reduced climate sensitivity of rock glaciers and their sustained cold-water input to mountain streams will likely provide a refuge for cold-water species as temperatures continue to rise, and these features merit a closer look at their role in a warming world.

Acknowledgments

We thank the many people who assisted with data collection over summers 2019–2021. A special thanks to Randall Bonnell for GPR processing guidance and State Forest State Park personnel for assistance with research permits. We would also like to thank Bob Anderson for insightful discussions about Colorado rock glaciers and Jeremy Caves Rugenstein for guidance with hydrochemistry. This material is based upon work supported by the National Science Foundation Graduate Research Fellowship awarded to BR under Grant No. 006784-00002, as well as funding awarded to B.R. by the American Alpine Club, the Geological Survey of America, and the Tobacco Root Geological Society. This material is based on services provided by the GAGE Facility, operated by UNAVCO, Inc., with support from the National Science Foundation, the National Aeronautics and Space Administration, and the U.S. Geological Survey under NSF Cooperative Agreement EAR-1724794. B.L. thanks the Mobility fellowship P2LAP2_191400 from the Swiss National Science Foundation for their support. This research was conducted in Colorado State Forest State Park, on the traditional lands of the Ute, Cheyenne, and Eastern Shoshone peoples.

Conflicts of Interest

The authors declare no conflicts of interest.

Data Availability Statement

The data that support the findings of this study are openly available in Lake Agnes Rock Glacier water quality at https://www.hydroshare.org/resource/c795eddf7e7f44e9b3efc25eb7a91d91/.

References

1. R. Agustina, M. R. Nicolás, E. B. Luis, B. Guido, and C. Eleonora, "Rock Glacier and Solifluction Lobes Groundwater as Nutrient Sources and Refugia for Unique Macroinvertebrate Assemblages in a Mountain Ecosystem of the North Patagonian Andes," *Aquatic Sciences* 86, no. 1 (2024): 11, https://doi.org/10.1007/s00027-023-01025-y.

2. S. Brighenti, S. Hotaling, D. S. Finn, et al., "Rock Glaciers and Related Cold Rocky Landforms: Overlooked Climate Refugia for Mountain Biodiversity," *Global Change Biology* 27, no. 8 (2021): 1504–1517, https://doi.org/10.1111/gcb.15510.

3. M. Huss, B. Bookhagen, C. Huggel, et al., "Toward Mountains Without Permanent Snow and Ice," *Earth's Future* 5, no. 5 (2017): 418–435, https://doi.org/10.1002/2016EF000514.

4. N. Pepin, R. S. Bradley, H. F. Diaz, et al., "Elevation-Dependent Warming in Mountain Regions of the World," *Nature Climate Change* 5, no. 5 (2015): 424–430, https://doi.org/10.1038/nclimate2563.

5. R. S. Anderson, L. S. Anderson, W. H. Armstrong, M. W. Rossi, and S. E. Crump, "Glaciation of Alpine Valleys: The Glacier–Debris-Covered Glacier–Rock Glacier Continuum," *Geomorphology* 311 (2018): 127–142, https://doi.org/10.1016/j.geomorph.2018.03.015.

6. S. Hotaling, M. E. Foley, L. H. Zeglin, et al., "Microbial Assemblages Reflect Environmental Heterogeneity in Alpine Streams," *Global Change Biology* 25, no. 8 (2019): 2576–2590, https://doi.org/10.1111/gcb.14683.

7. D. J. Isaak, M. K. Young, D. E. Nagel, D. L. Horan, and M. C. Groce, "The Cold-Water Climate Shield: Delineating Refugia for Preserving Salmonid Fishes Through the 21st Century," *Global Change Biology.* 21 (2015): 2540–2553, https://doi.org/10.1111/gcb.12879.

8. C. C. Muhlfeld, T. J. Cline, J. J. Giersch, et al., "Specialized Meltwater Biodiversity Persists Despite Widespread Deglaciation," *Proceedings of the National Academy of Sciences of the United States of America* 117, no. 22 (2020): 12208–12214, https://doi.org/10.1073/pnas.2001697117.

9. L. M. Tronstad, S. Hotaling, J. J. Giersch, O. J. Wilmot, and D. S. Finn, Headwaters Fed by Subterranean Ice: Potential Climate Refugia for Mountain Stream Communities? *bioRxiv*, 2019, https://doi.org/10.1101/788273.

10. N. Colombo, F. Salerno, S. Gruber, et al., "Review: Impacts of Permafrost Degradation on Inorganic Chemistry of Surface Fresh Water," *Global and Planetary Change* 162, no. August 2017 (2018): 69–83, https://doi.org/10.1016/j.gloplacha.2017.11.017.

11. J. R. Janke, S. Ng, and A. Bellisario, "An Inventory and Estimate of Water Stored in Firn Fields, Glaciers, Debris-Covered Glaciers, and Rock Glaciers in the Aconcagua River Basin, Chile," *Geomorphology* 296 (2017): 142–152, https://doi.org/10.1016/j.geomorph.2017.09.002.

12. D. Jones, S. Harrison, K. Anderson, and W. B. Whalley, "Rock Glaciers and Mountain Hydrology: A Review," *Earth-Science Reviews* 193, no. April (2019): 66–90, https://doi.org/10.1016/j.earscirev.2019.04.001.

13. M. Leopold, M. W. Williams, N. Caine, J. Völkel, and D. Dethier, "Internal Structure of the Green Lake 5 Rock Glacier, Colorado Front Range, USA," *Permafrost and Periglacial Processes* 22, no. 2 (2011): 107–119, https://doi.org/10.1002/ppp.706.

14. J. S. Munroe, "Distribution, Evidence for Internal Ice, and Possible Hydrologic Significance of Rock Glaciers in the Uinta Mountains, Utah, USA," *Quaternary Research (United States)* 90, no. 1 (2018): 50–65, https://doi.org/10.1017/qua.2018.24.

15. S. Rangecroft, S. Harrison, and K. Anderson, "Rock Glaciers as Water Stores in the Bolivian Andes: An Assessment of Their Hydrological Importance," *Arctic, Antarctic, and Alpine Research* 47, no. 1 (2015): 89–98, https://doi.org/10.1657/AAAR0014-029.

16. T. Wagner, S. Seelig, K. Helfricht, et al., "Assessment of Liquid and Solid Water Storage in Rock Glaciers Versus Glacier Ice in the Austrian Alps," *Science of the Total Environment* 800 (2021): 149593, https://doi.org/10.1016/j.scitotenv.2021.149593.

17. D. Barsch, *Rock-Glaciers: Indicators for the Present and Former Geoecology in High Mountain Environments*, vol. 16 (Springer-Verlag Berlin Heidelberg, 1996).

18. J. R. Giardino and J. Vitek, "The Significance of Rock Glaciers in the Glacial-Periglacial Landscape Continuum," *Journal of Quaternary Science* 3, no. 1 988 (1988): 97–103.

19. RGIK, "IPA Action Group Rock Glacier Inventories and Kinematics (Version 4.1)," *International Permafrost Association, Version* 1 (2022): 1–13.

20. I. Berthling, "Geomorphology Beyond Confusion: Rock Glaciers as Cryo-Conditioned Landforms," *Geomorphology* 131, no. 3–4 (2011): 98–106, https://doi.org/10.1016/j.geomorph.2011.05.002.

21. S. Monnier and C. Kinnard, "Reconsidering the Glacier to Rock Glacier Transformation Problem: New Insights From the Central Andes of Chile," *Geomorphology* 238 (2015): 47–55, https://doi.org/10.1016/j.geomorph.2015.02.025.

22. J. F. Shroder, M. P. Bishop, L. Copland, and V. F. Sloan, "Debris-Covered Glaciers and Rock Glaciers in the Nanga Parbat Himalaya, Pakistan," *Geografiska Annaler: Series A, Physical Geography* 82, no. 1 (2000): 17–31, https://doi.org/10.1111/j.0435-3676.2000.00108.x.

23. K. C. Burger, Jr., J. J. Degenhardt, Jr., and J. R. Giardino, "Engineering Geomorphology of Rock Glaciers," *Geomorphology* 31 (1999): 93–132.

24. W. Haeberli, "Creep of Mountain Permafrost: Internal Structure and Flow of Alpine Rock Glaciers," in *Mitteilungen Der Versuchsanstalt Fur Wasserbau, Hydrologie Und Glaziologie an Der Eidgenossischen Technischen Hochschule Zurich* (1985), 77.

25. W. Haeberli, B. Hallet, L. Arenson, et al., "Permafrost Creep and Rock Glacier Dynamics," *Permafrost and Periglacial Processes* 17, no. 3 (2006): 189–214, https://doi.org/10.1002/ppp.561.

26. C. Wahrhaftig and A. Cox, "Rock Glaciers in the Alaska Range," *Bulletin of the Geological Society of America* 70 (1959): 383–436.

27. C. Florentine, M. Skidmore, M. Speece, C. Link, and C. A. Shaw, "Geophysical Analysis of Transverse Ridges and Internal Structure at Lone Peak Rock Glacier, Big Sky, Montana, USA," *Journal of Glaciology* 60, no. 221 (2014): 453–462, https://doi.org/10.3189/2014JoG13J160.

28. H. Hausmann, K. Krainer, E. Brückl, and W. Mostler, "Internal Structure and Ice Content of Reichenkar Rock Glacier (Stubai Alps, Austria) Assessed by Geophysical Investigations," *Permafrost and Periglacial Processes* 18, no. 4 (2007): 351–367, https://doi.org/10.1002/ppp.601.

29. H. Maurer and C. Hauck, "Instruments and Methods: Geophysical Imaging of Alpine Rock Glaciers," *Journal of Glaciology* 53, no. 180 (2007): 110–120, https://doi.org/10.3189/172756507781833893.

30. K. Merz, H. Maurer, L. Rabenstein, T. Buchli, S. M. Springman, and M. Zweifel, "Multidisciplinary Geophysical Investigations Over an Alpine Rock Glacier," *Geophysics* 81, no. 1 (2016): WA147–WA157, https://doi.org/10.1190/geo2015-0157.1.

31. E. I. Petersen, J. S. Levy, J. W. Holt, and C. M. Stuurman, "New Insights Into Ice Accumulation at Galena Creek Rock Glacier From Radar Imaging of Its Internal Structure," *Journal of Glaciology* 66, no. 255 (2020): 1–10.

32. J. S. Harrington, A. Mozil, M. Hayashi, and L. R. Bentley, "Groundwater Flow and Storage Processes in an Inactive Rock Glacier," *Special Issue Canadian Geophysical Union 2018* 32, no. 20 (2018): 3070–3088, https://doi.org/10.1002/hyp.13248.

33. L. Liu, C. I. Millar, R. D. Westfall, and H. A. Zebker, "Surface Motion of Active Rock Glaciers in the Sierra Nevada, California, USA: Inventory and a Case Study Using InSAR," *Cryosphere* 7, no. 4 (2013): 1109–1119, https://doi.org/10.5194/tc-7-1109-2013.

34. K. Krainer, D. Bressan, B. Dietre, et al., "A 10,300-Year-Old Permafrost Core From the Active Rock Glacier Lazaun, Southern Ötztal Alps

(South Tyrol, Northern Italy),” *Quaternary Research* 83, no. 2 (2015): 324–335, https://doi.org/10.1016/j.yqres.2014.12.005.

35. D. J. Larsen, S. E. Crump, and A. Blumm, “Alpine Glacier Resilience and Neoglacial Fluctuations Linked to Holocene Snowfall Trends in the Western United States,” *Science Advances* 6, no. 47 (2020): eabc7661, https://doi.org/10.1126/sciadv.abc7661.

36. K. A. Refsnider and K. A. Brugger, “Rock Glaciers in Central Colorado, U.S.A., as Indicators of Holocene Climate Change,” *Arctic, Antarctic, and Alpine Research* 39, no. 1 (2007): 127–136, https://doi.org/10.1657/1523-0430(2007)39%5B127:RGICCU%5D2.0.CO;2.

37. S. T. Geiger, J. M. Daniels, S. N. Miller, and J. W. Nicholas, “Influence of Rock Glaciers on Stream Hydrology in the La Sal Mountains, Utah,” *Arctic, Antarctic, and Alpine Research* 46, no. 3 (2014): 645–658, https://doi.org/10.1657/1938-4246-46.3.645.

38. D. Jones, S. Harrison, K. Anderson, and R. A. Betts, “Mountain Rock Glaciers Contain Globally Significant Water Stores,” *Scientific Reports* 8, no. 1 (2018): 1–10.

39. N. Caine, “Recent Hydrologie Change in a Colorado Alpine Basin: An Indicator of Permafrost Thaw?,” *Annals of Glaciology* 51, no. 56 (2010): 130–134, https://doi.org/10.3189/172756411795932074.

40. K. Krainer, W. Mostler, and C. Spötl, “Discharge From Active Rock Glaciers, Austrian Alps: A Stable Isotope Approach,” *Austrian Journal of Earth Sciences* 100 (2007): 102–112.

41. T. S. Fegel, J. S. Baron, A. G. Fountain, G. F. Johnson, and E. K. Hall, “Biogeosciences Signatures of Glaciers and Rock Glaciers,” *Journal of Geophysical Research* 121, no. 3 (2016): 919–932, https://doi.org/10.1002/2015JG003236.

42. J. S. Harrington, M. Hayashi, and B. L. Kurylyk, “Influence of a Rock Glacier Spring on the Stream Energy Budget and Cold-Water Refuge in an Alpine Stream,” *Hydrological Processes* 31, no. 26 (2017): 4719–4733, https://doi.org/10.1002/hyp.11391.

43. M. W. Williams, M. Knauf, N. Caine, F. Liu, and P. L. Verplanck, “Geochemistry and Source Waters of Rock Glacier Outflow, Colorado Front Range,” *Permafrost and Periglacial Processes* 17 (2006): 13–33, https://doi.org/10.1002/ppp.535.

44. C. I. Millar and R. D. Westfall, “Distribution and Climatic Relationships of the American Pika (*Ochotona princeps*) in the Sierra Nevada and Western Great Basin, U.S.A.; Periglacial Landforms as Refugia in Warming Climates,” *Arctic, Antarctic, and Alpine Research* 42 (2010): 76–88, https://doi.org/10.1657/1938-4246-42.1.76.

45. G. Johnson, H. Chang, and A. Fountain, “Rock Glaciers of the Contiguous United States: GIS Inventory and Spatial Distribution Patterns,” September, 1–26, 2020.

46. J. R. Janke, “Colorado Front Range Rock Glaciers: Distribution of Topographic Characteristics,” *Arctic and Alpine Research* 39, no. 1 (2007): 74–83.

47. J. R. Janke, “Photogrammetric Analysis of Front Range Rock Glacier Flow Rates,” *Methods* 87 (2005b): 515–526.

48. J. R. Janke, “Long-Term Flow Measurements (1961–2002) of the Arapaho, Taylor, and Fair Rock Glaciers, Front Range, Colorado,” *Physical Geography* 26, no. 4 (2005a): 313–336, https://doi.org/10.2747/0272-3646.26.4.313.

49. S. E. White, “Rock Glacier Studies in the Colorado Front Range, 1961 to 1968,” *Arctic and Alpine Research* 3, no. 1 (1971): 43–64, https://doi.org/10.2307/1550382.

50. M. Leopold, G. Lewis, D. Dethier, N. Caine, and M. W. Williams, “Cryosphere: Ice on Niwot Ridge and in the Green Lakes Valley, Colorado Front Range,” *Plant Ecology and Diversity* 8, no. 5–6 (2015): 625–638, https://doi.org/10.1080/17550874.2014.992489.

51. S. R. Fassnacht, G. G. Patterson, N. B. H. Venable, et al., “How Do We Define Climate Change? Considering the Temporal Resolution of Niveo-Meteorological Data,” *Hydrology* 7, no. 3 (2020): Article 3, https://doi.org/10.3390/hydrology7030038.

52. J. M. O'Neill, *Geologic Map of the Mount Richthofen Quadrangle and the Western Part of the Fall River Pass Quadrangle, Grand and Jackson Counties, Colorado (Report 1291; IMAP)* (Denver, Colorado: USGS Publications Warehouse, 1981), https://doi.org/10.3133/i1291.

53. M. Cappucci, “Cameron Peak Fire Grows to Largest on Record in Colorado—The Washington Post,” The Washington Post, 2020, https://www.washingtonpost.com/weather/2020/10/15/cameron-peak-fire-colorado/.

54. R. Hudson and J. Fraser, “The Mass Balance (or Dry Injection) Method,” *Management* 9, no. 1 (2005): 6–12.

55. G. Langston, L. R. Bentley, M. Hayashi, A. Mcclymont, and A. Pidlisecky, “Internal Structure and Hydrological Functions of an Alpine Proglacial Moraine,” *Hydrological Processes* 25, no. 19 (2011): 2967–2982, https://doi.org/10.1002/hyp.8144.

56. T. Takasu and A. Yasuda, “Development of the Low-Cost RTK-GPS Receiver With an Open Source Program Package RTKLIB,” in *International Symposium on GPS/GNSS* (Jeju, Korea, November 4–6, 2009).

57. T. A. Scambos, M. J. Dutkiewicz, J. C. Wilson, and R. A. Bindschadler, “Application of Image Cross-Correlation to the Measurement of Glacier Velocity Using Satellite Image Data,” *Remote Sensing of Environment* 42, no. 3 (1992): 177–186, https://doi.org/10.1016/0034-4257(92)90101-O.

58. O. Conrad, B. Bechtel, M. Bock, et al., “System for Automated Geoscientific Analyses (SAGA) v. 2.1.4,” *Geoscientific Model Development* 8 (2015): 1991–2007, https://doi.org/10.5194/gmd-8-1991-2015.

59. J. S. Munroe and A. L. Handwerger, “Contribution of Rock Glacier Discharge to Late Summer and Fall Streamflow in the Uinta Mountains, Utah, USA,” *Hydrology and Earth System Sciences* 27, no. 2 (2023): 543–557, https://doi.org/10.5194/hess-27-543-2023.

60. C. Del Siro, C. Scapozza, M.-E. Perga, and C. Lambiel, “Investigating the Origin of Solutes in Rock Glacier Springs in the Swiss Alps: A Conceptual Model,” *Frontiers in Earth Science* 11 (2023): 1056305, https://doi.org/10.3389/feart.2023.1056305.

61. U. Nickus, H. Thies, K. Krainer, K. Lang, V. Mair, and D. Tonidandel, “A Multi-Millennial Record of Rock Glacier Ice Chemistry (Lazaun, Italy),” *Frontiers in Earth Science* 11 (2023): 1141379, https://doi.org/10.3389/feart.2023.1141379.

62. B. P. Ilyashuk, E. A. Ilyashuk, R. Psenner, R. Tessadri, and K. A. Koinig, “Rock Glacier Outflows May Adversely Affect Lakes: Lessons From the Past and Present of Two Neighboring Water Bodies in a Crystalline-Rock Watershed,” *Environmental Science and Technology* 48 (2014): 6192–6200, https://doi.org/10.1021/es500180c.

63. G. Brencher, A. L. Handwerger, and J. S. Munroe, “InSAR-Based Characterization of Rock Glacier Movement in the Uinta Mountains, Utah, USA,” *Cryosphere* 15, no. 10 (2021): 4823–4844, https://doi.org/10.5194/tc-15-4823-2021.

64. K. Merz, A. G. Green, T. Buchli, S. M. Springman, and H. Maurer. 2015. “A New 3-D Thin-Skinned Rock Glacier Model Based on Helicopter GPR Results From the Swiss Alps,” *Geophysical Research Letters* 42, no. 11: 4464–4472, https://doi.org/10.1002/2015GL063951.

65. H. Thies, U. Nickus, M. Tolotti, R. Tessadri, and K. Krainer, “Evidence of Rock Glacier Melt Impacts on Water Chemistry and Diatoms in High Mountain Streams,” *Cold Regions Science and Technology* 96 (2013): 77–85, https://doi.org/10.1016/j.coldregions.2013.06.006.

Supporting Information

Additional supporting information can be found online in the Supporting Information section.